第27卷 第1期
2005年3月

西 北 地 震 学 报
NORTHWESTERN SEISMOLOGICAL JOURNAL

Vol. 27 No. 1
March, 2005

3-dimensional Response of a Pile-ground System During Liquefaction and Flow Process of the Ground

SATO T[1], MATSUMARU T[2], MOON Y[3], ZHANG F[4], UZUOKA R[5]

(1. *Disaster Prevention Research Institute, Kyoto University, Uji, Kyoto* 6110011, *Japan*;
2. *Dept. of Civil Engineering, Kyoto University, Kyoto, Kyoto* 6068501, *Japan*;
3. *Civil Works Division, Samsung Corporation, Sungnam, Gyonggi* 463721, *Korea*;
4. *River Basin Research Center, Gifu University, Gifu, Gifu* 5011193, *Japan*;
5. *Dept. of Civil Engineering, Tohoku University, Sendai, Miyagi* 9808579, *Japan*)

Abstract: Loose saturated sand behaves as a solid before liquefaction but as a fluid when the excess pore water pressure reaches the initial confining stress, after which it recovers its strength. Those processes cannot be treated independently, but should be considered continuous processes that represent change from the solid to fluid state or from the fluid to solid state. Therefore, the total processes of the combined liquefaction—ground flow phenomenon should be treated as a series of processes of phase transformation between the solid and fluid states. In this paper, a simple constitutive equation for loose saturated sand was developed to be able to express the phase transformation between a solid and fluid during liquefaction and the ground flow phenomenon. This constitutive equation was used for a dynamic analysis of a pile—ground system, and its applicability investigated by comparing with the elasto—plastic constitutive equation.

Key words: Pile; Liquefaction; Ground flow phenomenon; Effective stress analysis

桩基系统在地基液化和土体流动过程中的三维响应

SATO T[1], MATSUMARU T[2], MOON Y[3], ZHANG F[4], UZUOKA R[5]

(1. 京都大学灾害防御研究所,宇治,京都 610011,日本;2. 京都大学土木工程系,京都,京都 6068501,日本;3. 三星集团土木工程部,Sungnam,京畿道 463721,韩国;4. 岐阜大学河流盆地研究中心,岐阜 5011193,日本;5. 东北大学土木工程系,仙台,宫城县 9808579,日本)

摘 要:松散的饱和砂土在液化之前可作为固体看待,但当过量的孔隙水压达到初始侧应力时它成为液体,之后又恢复其强度。这个过程不能各自单独处理,而应视为一个从固态到液态,或从液态到固态的连续变化过程。因此,整个伴随着地基液化——土体流动现象全过程应作为一个在固态和液态之间相变的系列过程。本文导出了一个简单的基本方程式,可以表达松散饱和砂土在液化和地基侧向滑移现象期间的固一液相转换。该基本方程式可用作桩基系统的动力分析,其适用性通过与弹塑性基本方程的比较得到验证。

关键词:桩基; 液化; 土体流动现象; 有效应力分析

中图分类号:TU441^{+}.6 **文献标识码**:A **文章编号**:1000—0844(2005)01—0022—08

收稿日期:2004-06-14

0 Introduction

The 1995 Hyogoken — Nambu earthquake, magnitude 7.2 (Richter scale), caused wide-spread liquefaction of almost all the reclaimed land in Kobe. This liquefaction caused significant damage in Kobe City. In particular, many pile foundations failed because of the deformation of the surrounding ground in liquefied ground. The main reason of damage to pile foundations in liquefied ground is lateral flow. Such a large horizontal displacement of soil by liquefaction and the ground flow phenomenon first was reported by Hamada et al. after a detailed aerial photographic survey made in Niigata City which was struck by a large severe earthquake in 1964. Based on reported results, there was horizontal permanent displacement of more than 10m on the bank of the Shinano River in Niigata City. Since then, the ground flow phenomenon caused by liquefaction has been a main topic of liquefaction research.

When saturated sand undergoes cyclic loading, pore water pressure increases until it equals the initial confining stress. As a result, the shear strength of the soil is lost. This is well known as the definition of liquefaction. Further, when liquefied ground undergoes a continuous external driving force, such as that caused by the inclination of its surface, the ground flows like a viscous fluid. As a result, there is large deformation of the surface laterally and damage to structures. This is the ground flow phenomenon. Finally the ground flow phenomenon that accompanies liquefaction ends, the liquefied sand recovers its stiffness, and shear stress increases rapidly as pore water pressure decreases. Consequently, the process of liquefaction and the ground flow phenomenon can be classified in three parts: the solid state before the onset of liquefaction, the fluid state after liquefaction, and the recovered solid state owing to dissipation of the excess pore water pressure and dilatancy caused by development of large shear strain. Therefore, the total processes of the combined liquefaction — ground flow phenomenon should be treated as a series of processes of phase transformation between the solid and fluid states.

We have used mechanical and numerical modeling of seismic liquefaction and the ground flow phenomenon in saturated loose sandy soil based on elasto—plastic and viscous fluid constitutive equations. A simple constitutive equation was developed to unify these phase transformations of saturated loose sand. It combines the cyclic elasto—plastic behavior of sand and the Newtonian viscous fluid characteristics of liquefied sand by defining the phase transformation function. This constitutive equation provides a unified constitutive equation for the characterization of the entire process of liquefaction from the initial to post — liquefaction state. We applied this constitutive equation to analyze the dynamic behavior of a pile — ground system, and to simulate dynamic interaction between a pile and liquefied ground accompanying a flow phenomenon. Its efficiency is investigated by comparing with simulated results obtained by using the elasto—plastic constitutive equation.

1 Concept of the Proposed Constitutive Equation

Based on solid mechanics, the relationship between the total stress and effective stress of a mixture using the component of pore water pressure is

$$\sigma_{ij} = \sigma'_{ij} + p\delta_{ij} \tag{1}$$

where σ_{ij}, σ'_{ij}, p are the total stress tensor, effective stress tensor, and pore water pressure, and δ_{ij} is the Kronecker delta.

When the solid skeleton of a mixture is assumed to be an elasto-plastic body, the effective stress, σ'_{ij}, in Equation (1) becomes the stress, σ^{ep}_{ij}, of the elasto—plastic body. And Equation (1) becomes

$$\sigma_{ij} = \sigma^{ep}_{ij} + p\delta_{ij} \tag{2}$$

In contrast, the total stress of the viscous fluid in fluid mechanics generally is described as

$$\sigma_{ij} = \sigma^{vf}_{ij} + p\delta_{ij} \tag{3}$$

where σ^{vf}_{ij} is the viscous resistance stress tensor in the viscous fluid.

A comparison of Equations (2) and (3) shows that the component in which the pore water pressure is subtracted from the total stress tensor expresses the effective stress tensor in Equation (2) and the viscous stress tensor in Equation (3). This means that the viscous stress tensor in fluid mechanics coincides with the effective stress tensor concerned with the stiffness of a soil skeleton of a mixture.

Using this relationship, we propose a simple constitutive equation for loose saturated sand that expresses the phase transformation between the solid and fluid states during the liquefaction and ground flow processes. The newly proposed constitutive equation is called the fluidal-elasto-plastic constitutive equation and defined as Equation (4), and a schematic view of the constitutive equation is shown in Fig. 1.

$$\sigma_{ij} = (1-\alpha)\sigma_{ij}^{ep} + \alpha\sigma_{ij}^{vf} + p\delta_{ij} \tag{4}$$

where α is the phase transformation — controlling function. The stress, σ_{ij}^{ep}, is evaluated by the cyclic elasto—plastic constitutive equation. The relationship is written as follows by means of the incremental formulation

$$d\sigma_{ij}^{ep} = D_{ijkl}^{ep}\, d\varepsilon_{kl} \tag{5}$$

where D_{ijkl}^{ep} is the fourth-order isotropic tensor concerned with the stress-strain relationship for the elasto-plastic constitutive equation, and $d\varepsilon_{kl}$ is the strain tensor increment. The stress, σ_{ij}^{vf}, is evaluated by a Newtonian viscous fluid constitutive equation as

$$\sigma_{ij}^{vf} = D_{ijkl}^{vf}\dot{\varepsilon}_{kl} = 2\mu'\dot{\varepsilon}_{ij} + \lambda'\dot{\varepsilon}_{kk}\delta_{ij} \tag{6}$$

where D_{ijkl}^{vf} is the fourth-order isotropic tensor concerned with the stress-strain rate relation for the Newtonian viscous fluid, $\dot{\varepsilon}_{kl}$ is the strain rate tensor, and μ', λ' are the viscous and the second viscous coefficients.

In this paper, the phase transformation function, α, is a function of the effective stress through the process of liquefaction, ground flow and recovery of stiffness. The phase transformation function is expressed by

$$\alpha = 1.0 + \tan h(a\cdot(1-\sigma'_m/\sigma'_{m0}) - b) \tag{7}$$

where σ'_m, σ'_{m0} are current and initial mean effective stresses, $1-\sigma'_m/\sigma'_{m0}$ is the relative effective stress ratio (R. E. S. R.) and a, b are parameters.

This relationship between α and R. E. S. R. is shown in Fig. 2. When R. E. S. R. is more than 0.9, the value of α rapidly increases, and when the value reaches 1.0, α becomes 1.0 reversibly. α then rapidly decreases with recovery of the mean effective stress caused by seepage and dilatancy. Actuation of the fluid behavior modeled by a Newtonian viscous fluid is limited to a region in which the mean effective stress is very small.

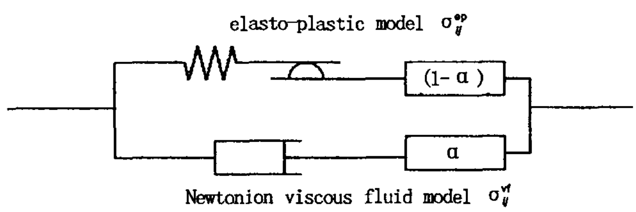

Fig. 1 Concept of the fluidal—elasto—plastic model.

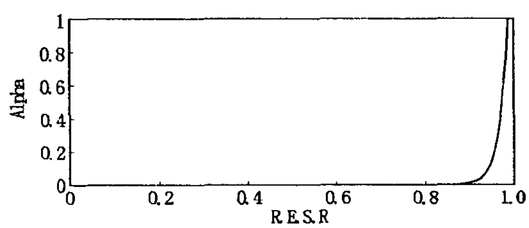

Fig. 2 Relationship between α and R. E. S. R.

2 Numerical Formulation of the Proposed Constitutive Equation

A field equation based on the proposed constitutive equation is derived from Biot's mixture theory for a two — phase porous medium composed of the soil skeleton and pore water. The dynamic motion of the proposed constitutive equation is described by the u-p formulation introduced by Oka et al.. The equilibrium equation and the continuity equation are derived as

$$\rho\ddot{u}_i^s = \frac{\partial\sigma_{ij}}{\partial x_i} + \rho b_i \tag{8}$$

$$\frac{K}{\gamma_w}\left(\rho^f\ddot{\varepsilon}_{ii}^s - \frac{\partial^2 p_d}{\partial x_i^2}\right) - \dot{\varepsilon}_{ii}^s + \frac{n}{K^f}\dot{p}_d = 0 \tag{9}$$

where ρ is the overall density, $\ddot{u}_i^s$ is the acceleration of the solid, b_i is the body force, k is the coefficient of permeability, γ_w is the unit weight of the fluid, ρ^f is the density of the fluid, ε_{ii}^s is the volumetric strain of the solid, n is porosity and K^f is the bulk modulus of the fluid.

The finite element method based on the u—

p formulation gives the discretized formulation for the equilibrium equation:

$$[M]\{\ddot{u}_N\} + ((1-\alpha)[C^{ep}] + \alpha[C^{vf}])\{\dot{u}_N\} + (1-\alpha)[K]\{\Delta u_N\} + \{K_v\}p_{dE} = \{F_d\} - \{R_{d|t}\} \tag{10}$$

where $[M]$,$[K]$,$[C^{ep}]$,$[C^{vf}]$ are the mass matrix, stiffness matrix of the elasto—plastic model, Rayleigh damping matrix, and matrix for the relation between the stress and strain rate of the Newtonian viscous fluid model, and $\{K_v\}$, $\{F_d\}$, $\{R_t\}$ are the transformation vector from nodal displacement to volumetric strain, the vector of the external body force caused by inertia, and vector of the residual force in the previous time step.

In contrast, for the continuity equation (Equation (9)), the pore water pressure is discretized by the finite different method in the space domain, and the discretized formulation for the continuity equation is

$$\rho^f\{K_v\}^T\{\ddot{u}_N\} - \frac{\gamma_w}{k}\{K_v\}^T\{\dot{u}_N\} - \alpha' p_{dE} + \sum_{i=1}^{4}\alpha' p_{dE_i} + A\dot{p}_{dE} = 0 \tag{11}$$

where α', α'_I are coefficients of pore water pressure approximated by a finite different mesh between the central and neighboring elements, p_{dE_i} is the central pore water pressure on the neighboring element and A is the coefficient for compressibility of the fluid. Furthermore, Equations (10) and (11) can be discretized by the Newmark — β method for the time domain.

3 A Hybrid Element and AFD Model

In simulating a pile, the usual method in the finite element analysis is to use a beam element that is known to be a non—volume element. If the area and volume of piles are not considered properly, we face to some difficulties to analyze the interaction between the piles and the ground that is heavily dependent on the geometry of the piles. For this reason, a hybrid element is implemented to simulate the pile behavior. In this paper, a pile is modified a hybrid element that consists of a beam element and solid elements as shown in Fig. 3. The stiffness of the pile is shared by the beam element and several solid elements in such a way that the bending stiffness of pile EI is equal to the sum of the bending stiffness of beam element $(EI)_{beam}$ and solid elements $(EI)_{solid}$. The sharing ratio between the stiffness of beam element and the solid element should be determined in such a way that the mechanical behavior of the cantilever beam simulated by a single beam element and the hybrid elements will be the same. In this paper, the sharing ratio between the stiffness of the beam element and the solid elements is selected as 9 to 1.

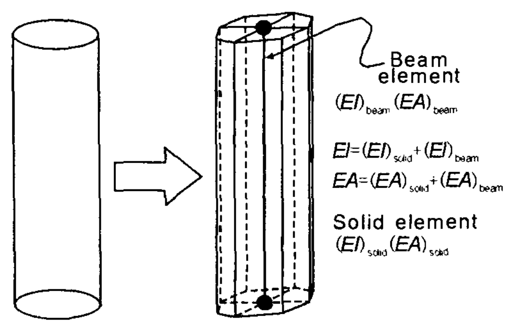

Fig. 3　Hybrid element.

AFD (Axial Force Dependent) model is proposed for reinforced concrete material (RC material). By taking the plane — section assumption, that is, when an RC member is subjected to a biaxial bending, axial force, and shear forces, any section along the member longitudinal axis is kept as a plane, this model can properly take into consideration the interactions among biaxial bending and axial forces. The stress — strain relations of reinforcement and concrete are shown in Fig. 4.

4 Numerical Simulation of a Pile-Ground System

4.1 Analytical conditions

For understanding behavior of the proposed constitutive equation, dynamic behavior of a pile-ground system in the liquefied ground accompanying the ground flow were simulated by using the fluidal-elasto-plastic constitutive equation and elasto-plastic constitutive equation. Three types of pile-ground system (CASE1; a single pile with liquefied ground, CASE2; a pile in the liquefied ground covered by unliquefied clay layer, CASE3; 4 piles with liquefied ground) are considered.

Fig. 5 shows the finite element models. The liquefiable soil for the all cases, composed of Silica NO. 8 ($D_{50}=0.24$, uniformity coefficient $U_c=1.92$, $e_{max}=1.251$, $e_{min}=0.706$) with a relative density of about 40% and fully saturated, is assumed to be filled in a model ground with the dimensions of 5.0 m high. And the pile (PHC—A) with 0.5 m in diameter and 6.0 m in length, is placed in the center of the model ground with 4% of inclination.

We use an 8-node isoparametric solid elements and beam elements. As a boundary condition, all nodes at the bottom are fixed, and the nodes at the boundary of X-Z plane are fixed only in Y-direction. At the both edge boundaries in X-direction - which is the flow direction, equi-displacement elements with 100 m width were installed, which behave as a uniformly deposited ground at both boundary and decrease the influence of boundary condition. The pile is fixed at the bottom and at the top.

Fig. 6 shows the used input acceleration time history. Acceleration is inputted in the Y-direction and the ground is liquefied completely about at 4 seconds after the earthquake motion input. The liquefied ground flows in the X-direction due to the inclination of the model ground. Table 1 gives the constitutive parameters of clay and liquefiable soil. The parameters of the pile described by AFD model are listed in Table 2.

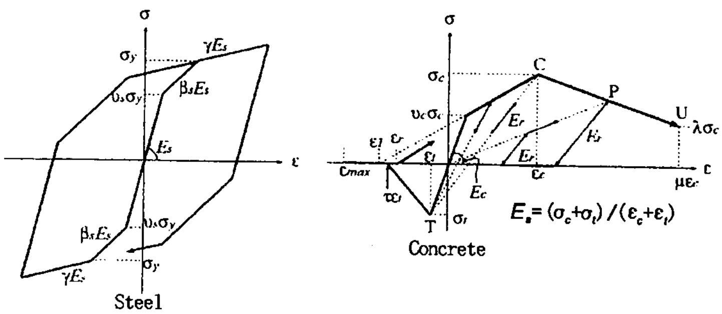

Fig. 4 Nonlinear properties of reinforcement and concrete.

Table 1 Parameters for sandy soil and clay

Parameter	Sand	Clay	Parameter	Sand	Clay
Initial void ratio e_0	1.143	1.75	Hardening parameter B_0	3 200.0	3 000.0
Compression index λ	0.025	0.01	Hardening parameter B_1	32.0	100.0
Swelling index κ	0.002 5	0.000 5	Dilatancy parameter D_0	3.50	0.0
Initial shear modulus G_0/σ'_{m0}	43.0	524.0	Dilatancy parameter n	1.10	0.0
Phase transformation stress ratio M_m	0.909	0.980	Reference strain for plastic γ_r^P	0.001	1 000.0
Failure stress ratio M_f	1.308	0.980	Reference strain for elastic γ_r^E	0.006	1 000.0

Table 2 Parameters for PHC—A pile

Parameter		Parameter	
External diameter/mm	500	Young's modulus of concrete/MPa E_c	$2.45\cdot10^4$
Internal diameter/mm	420	Compressive strength of concrete/MPa σ_c	78.4
Overburden of reinforcement/mm	40	Tensile strength of concrete/MPa σ_t	4.7
Diameter of reinforcement/mm	7.1	Young's modulus of steel/MPa E_s	$2.06\cdot10^5$
Number of reinforcement	10	Yielding strength of steel/MPa σ_y	1 270.0

4.2 Results of analysis and discussions

Fig. 7 shows the simulated results of a CASE1, which are the time histories of the relative effective stress ratio (R. E. S. R.) and phase transformation function, α, at the point of element E(Fig. 5) for both cases of using the elasto-plastic and fluidal—elasto—plastic constitutive equations. The simulated result of time history of the R. E. S. R. (Fig. 7(a)) indicates that liquefaction occurred at about 4 seconds because the R. E. S. R. is

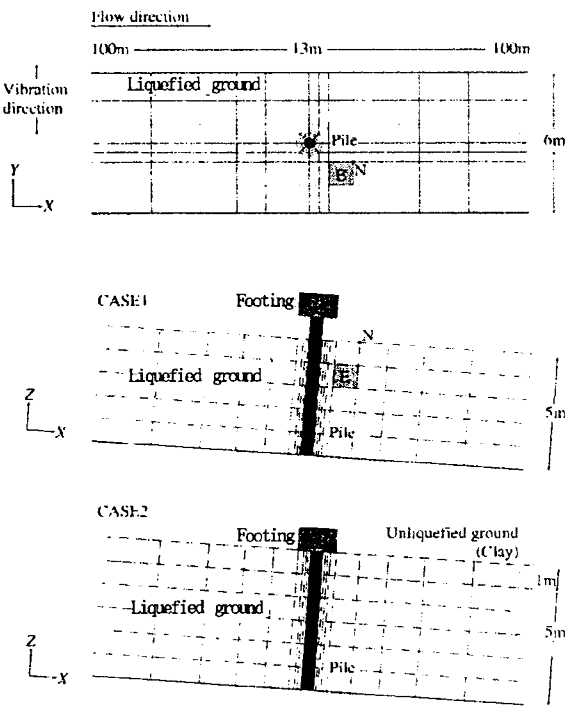

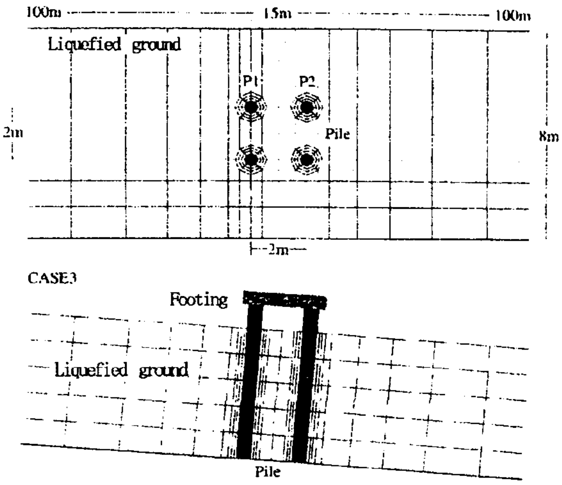

Fig. 5 Finite element models.

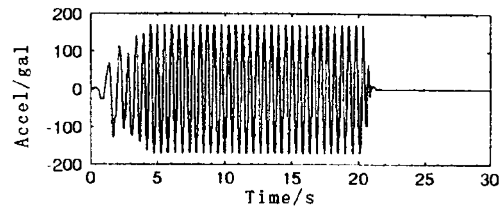

Fig. 6 Input acceleration.

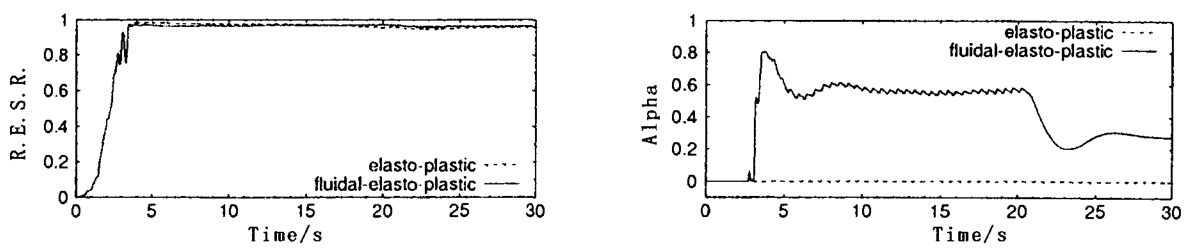

(a) R. E. S. R　　(b) Alpha

Fig. 7　Time histories of R. E. S. R. and alpha in CASE1.

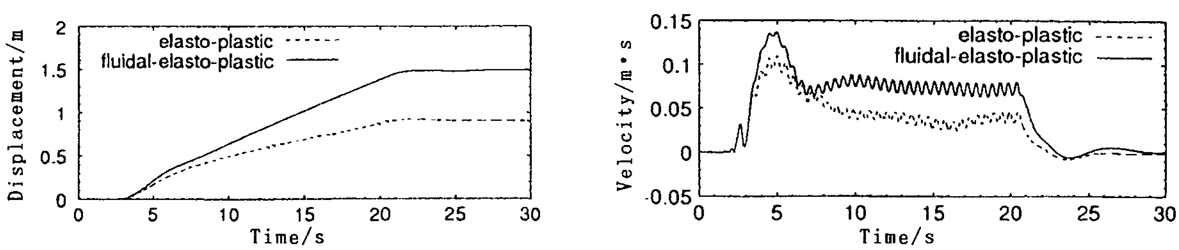

(a) Displacement　　(b) Velocity

Fig. 8　Time histories of displacement and velocity.

almost reached 1. 0 at this time. As the phase transformation function in the fluidal-elasto-plastic constitutive equation is increased, the part of the stress contributed from the Newtonian viscous fluid is increased. In the time history of phase transformation function (Fig. 7(b)), the phase transformation, which starts form solid state, turns to fluid state and returns to solid state, can be rigorously expressed.

Fig. 8 shows the time histories of the horizontal displacement and velocity of lateral flow at the node N (Fig. 5) for cases using the elasto—plastic and fluidal—elasto—plastic constitutive equations. Comparing the simulated results of the displacement and velocity, the values obtained by using the fluidal—elasto—plastic constitutive equation is larger than those by the elasto-plastic constitutive equation. This indicates that the fluidal characteristic of liquefied ground is expressed more effectively by the fluidal — elasto — plastic constitutive equation than the elasto—plastic constitutive equation.

The distributions of maximum curvature (r. m. s. of curvature in X and Y direction) of a pile, for CASE1, CASE2 and pile P1 and P2 of CASE3, are shown in Fig. 9. Large curvatures occurred at the top and the head of pile because the pile is fixed at the bottom and at the top. In CASE1 and CASE3, the maximum curvature obtained by using the fluidal—elasto—plastic constitutive equation is smaller than that by the elasto-plastic constitutive equation (Fig. 9(a), (c) and (d)). On the other hand, in CASE2, the result is opposite, which means that the curvature obtained by using the fluidal elasto — plastic constitutive equation is larger (Fig. 9(b)).

Fig. 10 shows the hysteretic loop of the moment-curvature relation of the pile at bottom in CASE1 and CASE2. In CASE1, although a large hysteretic loop occurs for the elasto-plastic constitutive equation, such a big loop does not occur and the pile behaves elastically for the fluidal-elasto-plastic constitutive equation. In CASE2, the pile behaves plastically for both constitutive equation, and the moment and curvature simulated with the fluidal — elasto — plastic constitutive equation becomes larger.

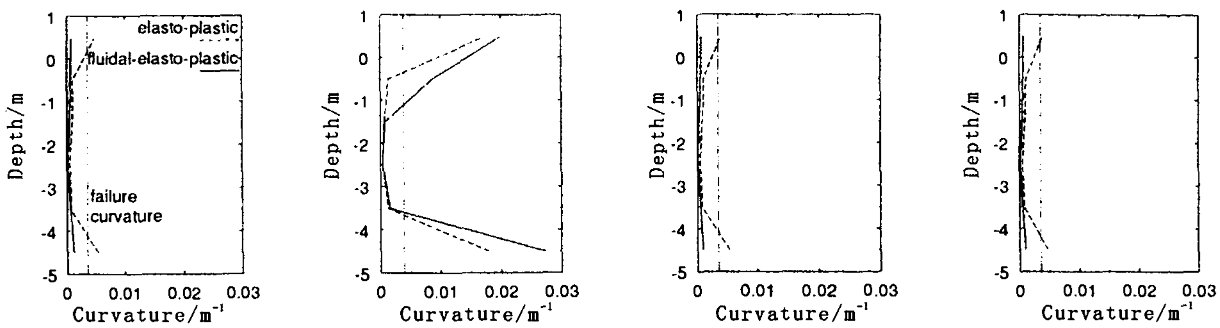

(a) CASE1 (b) CASE2 (c) CASE3-P1 (d) CASE3-P2

Fig. 9 Distribution of maximum curvature.

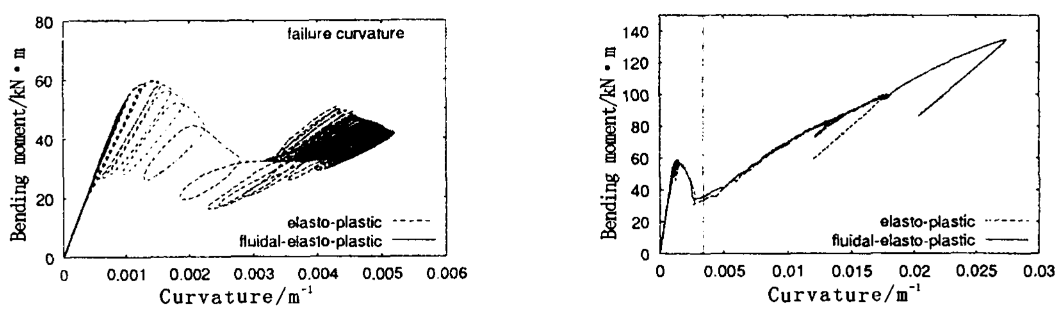

(a) CASE1 (b) CASE2

Fig. 10 Moment—curvature relations of pile in CASE1 and CASE2.

To discuss the reason of these differences among cases, the time histories of curvatures in CASE1 and CASE2 are shown in Fig. 11. In CASE1, the curvature simulated by the elasto-plastic constitutive equation increases rapidly at 4—8 second, but the result by the fluidal—elasto—plastic constitutive equation is nearly constant. In this time period, liquefaction occurs (Fig. 7(a)) and the velocity of the ground has the maximum value (Fig. 8(b)). Therefore, the curvature is influenced by the difference of the phase of liquefied soil. In CASE2 (Fig. 11(b)), though the curvature obtained by the elasto — plastic constitutive equation is nearly constant after 10 second, the result by the fluidal — elasto — plastic constitutive equation increases even after this time. As can be seen in Fig. 8(b), the velocity and total displacement of ground simulated by the fluidal — elasto — plastic constitutive equation is larger. So, in the case of clay layer existing, this layer slides on the liquefied layer, and then the pile would be affected by the gravity force caused by the unliquefied clay layer.

Fig. 12 shows the ground displacement around the pile for CASE1 and CASE3. In any case and at

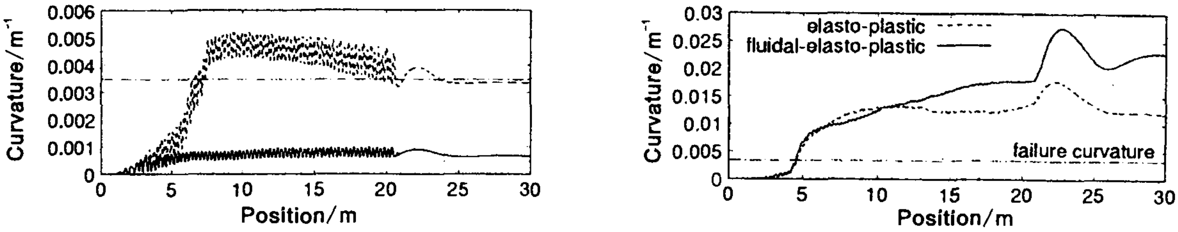

(a) CASE1 (b) CASE2

Fig. 11 Time histories of curvature at bottom in CASE1 and CASE2.

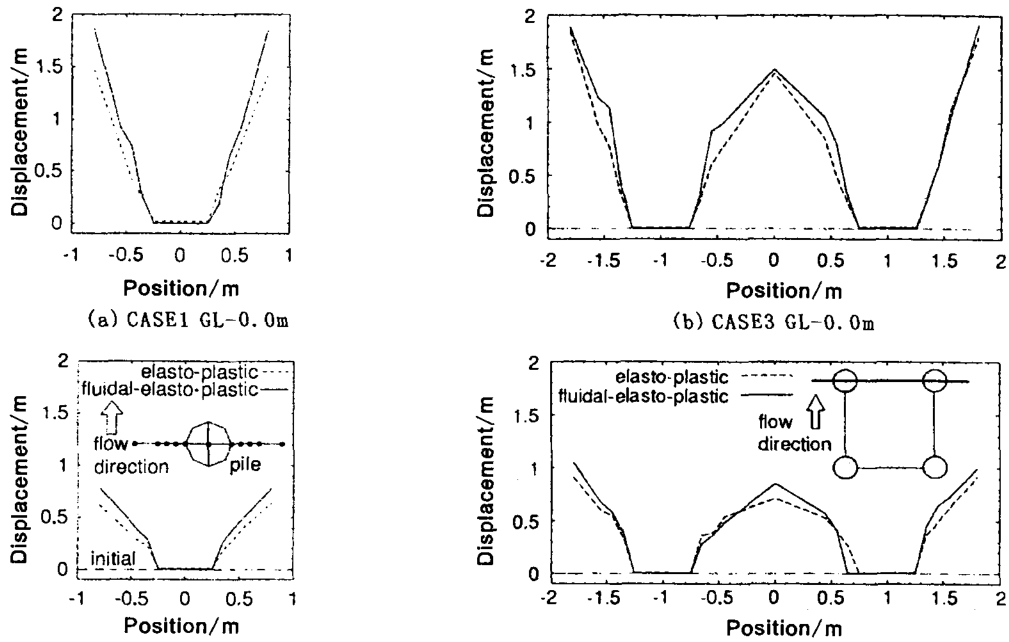

(a) CASE1 GL-0.0m (b) CASE3 GL-0.0m

(c) CASE1 GL-4.0m (d) CASE3 GL-4.0m

Fig. 12 Displacement of ground around the pile in CASE1 and CASE3.

any position, the ground simulated with the fluidal-elasto-plastic constitutive equation moves larger to downward of the inclination than that with the elasto-plastic constitutive equation.

5 Conclusion

The process of liquefaction and ground flow phenomenon is divisible into three phases: the solid state before onset of liquefaction, the fluid state of the liquefied soil, and the recovered solid state produced by dissipation of excess pore water pressure. Changes in the three phases are continous not separate phenomena. Liquefaction and the flow phenomenon should both be considered as combination of solid and fluid behaviors. We developed a simple constitutive equation with which to simulate the dynamic response of saturated loose sand by combining a cyclic elasto-plastic constitutive equation based on the solid mechanism and a Newtonian viscous fluid constitutive equation based on fluid mechanism through a phase transformation function.

The validity of our proposed constitutive equation was tested by conducting 3-dimensional effective stress analysis to three pile-ground systems. Compared with the results obtained by the elasto-plastic constitutive equation, the maximum displacement and velocity of ground become larger, when the ground flow phenomenon is taking into account. The pile response becomes large for the case without constrained layer on the ground surface but smaller for the case with constrained clay layer, but in both cases pile behavior is influenced strongly by the flow phenomenon when using the fluidal-elasto-plastic constitutive equation. The results calculated by using the fluidal elasto—plastic constitutive equation explain better the pile-ground system behavior during liquefaction and following ground flow process.

（下转 35 页）

House of Irkutsk University, 1994. 97(in Russian).
[5] Medvedev S V. Estimation of earthquake intensity. Epicentral zone of earthquakes[M]. Moscow: Nauka, 1978, 108－117(in Russian).
[6] Potapov V A, Dzis L V. Intensity of macroseismic field to predict effects on the ground－construction systems[J]. Earthquake－resistant construction, 2001, (6): 17－21(in Russian).
[7] Potapov V A, Ivanov F I. Intensity and seismic effect of earthquakes[J]. Earthquake－resistant construction, 1999, (5): 40－42(in Russian).
[8] Riznitcheno Yu V. Problems of seismology: Selected works [M]. Moscow: Nauka, 1985. 408(in Russian).
[9] Savarensky E F. Seismic waves[M]. Moscow: Nedra, 1972. 296(in Russian).
[10] Sadovsky M A. Selected works. Geophysics and physics of explosions[M]. Moscow: Nauka, 1999. 335(in Russian).
[11] Shebalin N V. On evaluation of seismic intensity. Seismic scale and methods of measurements of seismic intensity[M]. Moscow: Nauka, 1975. 87－109(in Russian).
[12] Timoshenko S P, Goodier J N. Theo

（上接29页）

[Reference]

[1] Sato T, Moon Y, Uzuoka R. Unified analysis of liquefaction and the ground flow phenomenon by the fluidal elasto plastic constitutive equation[J]. International Journal for Numerical and Analytical Methods in Geomechanics(under examination).
[2] Oka F, Yashima A, Tateishi A, et al.. A cyclic elasto－plastic constitutive model for sand considering a plastic strain dependency of the shear modulus[J]. Geotechnique, 1999, **49** (5): 661－680.
[3] Oka F, Yashima A, Shibata T, et al.. FEM－FDM coupled liquefaction analysis of a porous soil using an elasto－plastic model[J]. Applied Scientific Research, 1994, **52**: 209－245.
[4] Zhang F, Yashima A, Kimura M, et al.. 3－D FEM analysis of laterally cyclic loaded group－pile foundation based on an axial－force dependent hysteretic model for RC. Proc. of Int. Conf. on Geotech. and Geological Engrg., 2000(CD－ROM).